Pulse Buildup Dynamics of an Actively Mode-Locked Laser Diode Array in the External Cavity

Chi-Luen Wang, Jahn-Chung Kuo, C.-S. Chang, and Ci-Ling Pan

***Abstract*—Dynamic pulse evolution characteristics of an actively mode-locked laser diode array in the external cavity have been investigated. Numerical calculations based on modified traveling-wave rate equations reproduce experimentally observed pulse and spectral width evolution and show that the buildup time is about 45 round-trips. We have also performed a theoretical analysis to understand which of the laser operating parameters would affect the buildup dynamics. It is shown that either higher dc bias current or larger radiative recombination coefficient (which is inversely proportional to the excited-state lifetime) will render the laser exhibiting shorter steady-state pulse width and faster evolution to the steady state. Other parameters affecting the buildup, but to a lesser extent, include the radio-frequency (RF) modulation current, spontaneous emission coefficient, and gain coefficient. The power reflectivities of the output mirror and the antireflection coated diode facet, on the other hand, have little effect on the pulse width and buildup time for *single* pulse generation.**

I. INTRODUCTION

RECENTLY, SEVERAL GROUPS have investigated the buildup dynamics of mode-locked laser systems as the laser output evolved from noise bursts to steady state picosecond and femtosecond pulses [1]–[6]. It is hoped that, through these studies, one can elucidate the pertinent pulse shaping mechanisms. The buildup times for different types of mode-locked lasers are found to be quite different: The colliding-pulse mode- locked (CPM) ring dye lasers evolves to the steady state in about 1300 to 1500 round-trips [1], [2]. The buildup time for a synchronously pumped *R6G* dye laser is ≈800 round-trips [3]. For additive-pulse mode-locked (APM) or self-starting passively mode- locked Ti:sapphire lasers with intra-cavity saturable absorber, several tens of thousand round-trips are required [4]–[6]. The dynamics of AM mode-locked Ti:Al_2O_3 laser was analyzed theoretically by Reddy and Tatum [7]. Recently Ruan *et al.* [8] studied the pulse evolution in cw femtosecond Cr^{3+}:$LiSrAlF_6$ lasers mode-locked with MQW saturable absorbers. They found that the pulse duration shortened rapidly within the first millisecond as the mode-locking mechanism developed the pulse train. Once mode-locked pulses were formed and the absorption was saturated, a further period of ≈800 ms is required for the laser to settle at its steady state wavelength although the pulse duration is already determined.

A number of authors have also investigated the pulse buildup dynamics of semiconductor lasers. Lau and co-workers [9] showed that the time constant for buildup in passively mode-locked monolithic quantum-well semiconductor lasers is on the order of 3.5 ns, or ≈175 round-trips. This is significantly longer than the turn- on and turn-off time for comparable cw lasers. They also predict that, to decrease the pulse buildup time, the photon lifetime should be decreased and the gain, modulation of the gain and the ratio of the mode-locking frequency to the gain bandwidth should be increased. Experimentally, AuYeung *et al.* [10] was the first to show that the buildup time for an actively mode-locked double-heterostructure GaAlAs laser was ≈30 round-trips. The accuracy of their experimental results, however, was limited by the bandwidth of the detection system. The evolution process could not be resolved. In a numerical study, Demokan [11] estimated that the buildup time of an actively mode-locked AlGaAs–GaAs laser with one *perfectly antireflection (AR)*-coated facet would be ≈150 round-trips. Later, Blixt and Krotkus [12] showed both theoretically and experimentally that an actively mode-locked InGaAsP buried- heterostructure laser diode in the external cavity reached its steady state in 40 to 50 round-trips. On the other hand, numerical calculations of Bowers *et al.* [13] yielded a relatively slow buildup time of 62 ns, or nearly a 1000 roundtrips for their short-external cavity actively mode-locked InGaAsP laser modulated at 16 GHz.

Broad area or phase-locked array of laser diodes generating impressively high output power are now commercially available. Active mode-locking of a laser diode array with linear [14] or ring [15] external cavities have also been reported. The pulses generated were 61 and 26-ps wide with peak powers of 1.1 W and 30 mW, respectively. Recently, we have presented detailed experimental data on both the temporal and spectral evolution of picosecond pulses generated by an actively mode-locked laser diode array in an external cavity [16]. During the first 40 ns after the laser onset, the pulse width shortened quickly and approached the steady state 45 ps pulse width in approximately 100 ns, or 45 roundtrips. Concurrently the number of clusters of the longitudinal-mode spectrum reduced and approached a steady-state spectral distribution with the pulse energy mainly distributed among a few clusters near the line center. In this paper, a simple model based on modified

Manuscript received October 21, 1992; revised October 7, 1994. This work was supported in part by the National Science Council of the Republic of China under Grants NSC80-0 417-E009-05, -17 and NSC81-0 417-E049-629, -630.

The authors are with the Institute of Electro-optical Engineering, National Chiao Tung University, Hsinchu, Taiwan 300, R.O.C.

IEEE Log Number 9408596.

0018-9197/95$04.00 © 1995 IEEE

traveling-wave rate equations was developed which yielded numerical results in good agreement with experimentally observed dynamic pulse evolution behavior of this laser. We have also investigated theoretically significant laser operating parameters affecting the buildup time.

II. Traveling-wave Rate Equation Analysis

The dynamics of phase-locked semiconductor laser arrays has been previously investigated by Wang and Winful [17] using time-dependent coupled mode theory. They found that the evolution of the total intensity emitted in a single pulse by a ten- stripe array resembled that of single-stripe semiconductor laser after a few nanoseconds. This implies that even though we have adopted a simplified theoretical model appropriate for a single-stripe laser in the following, it is expected to be valid for describing the evolution characteristics of a phase-locked laser-diode array, as long as we are looking at time intervals longer than a few nanoseconds after the laser onset, i.e., a couple of round-trips for our laser configuration (round-trip time =2.309 ns). In view of excellent agreements of our calculation results with experimental observations, to be described in Section III, the simplification is justified.

For our analysis, we consider the laser configuration as shown in Fig. 1, which is identical to that of our experiment [16]. The laser diode array has a high- reflectivity (HR) coating of 95% on the back facet and an AR coating on the front facet. The output of the laser diode from the AR-coated facet was coupled through the optical components, e.g., the microscope-objective and cylindrical lens or graded-index lens, to an external cavity which is terminated by an output mirror. Our theoretical approach is equivalent to that of Bowers *et al.* [13] and basically an extension of the time-domain model first introduced by Demokan [11]. One modification is taking into account the finite reflectivity of the AR-coated diode facet. The residue reflectivity of the AR-coated facet of our laser, however, was fairly low ($R \cong 0.1\%$). Thus we can assume a random phase relationship between the reflected primary pulse from the AR-coated facet and the trailing pulse. The photon fluxes can thus be summed directly, i.e., the rate equations for the photon flux is expected to provide reasonably accurate results. Residue multiple reflections between the two facets of the chip, however, will cause the output spectrum of the actively mode-locked laser diode array exhibiting multiple clusters of longitudinal modes. For analysis of spectral evolution, we thus divide the laser output spectrum into $2M+1$ clusters, where M is an integer. Furthermore, the three dimensional problem is reduced to one dimensional after averaging over lateral coordinates. Since the steady-state pulse width for this laser is fairly long (≈ 45 ps), we have neglected the self phase modulation (SPM) effect due to gain-saturation induced index changes in the active medium. Similarly, pulse broadening due to group velocity dispersion (GVD) is also neglected. It will be shown in Section III that the change in carrier density, ΔN is -3×10^{16} cm^{-3} right after emission of the peak of the optical pulse in each modulation period (see Fig. 2). In comparison, Lowery [18] predicted a change in carrier density as large as 60×10^{16} cm^{-3}

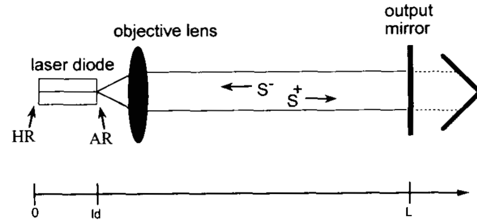

Fig. 1. Configuration of an actively mode-locked laser diode array in an external cavity. S^+ and S^- denote the photon densities propagate in the positive and negative x-directions, respectively.

when a 16 ps pulse passes through a laser diode amplifier. The difference is nonetheless plausible: In order to generate *single-pulse* output, the actively mode-locked laser diode must operate near threshold. If the laser pulse is relatively broad, gain-saturation and the associated spectral shift or chirping in the laser is not as substantial as that for amplifiers [19]. It is thus a good first approximation to neglect carrier or gain-saturation induced changes of index of refraction in our calculation, for the spectral shift or chirping of our laser is estimated to be small (a few GHz) compared to the FWHM of the pulse spectrum (see the inset of Fig. 3(b), about 1 THz). The resulting modified rate equation for the electron density $N(x,t)$ is then

$$\frac{\partial N(x,t)}{\partial t} = \frac{J(t)}{ed} - BN^2(x,t) - [N(x,t)-N_0]\sum_{i=-M}^{M} G_i[S_i^+(x,t)+S_i^-(x,t)] \tag{1}$$

where x is the distance along the direction of light propagation; e is the electronic charge; d is the thickness of the active layer; B is the radiative recombination coefficient; N_0 is the electron density for transparency; $S_i^+(x,t)$; and $S_i^-(x,t)$ are the sum of forward and backward traveling photon densities of the longitudinal modes in the ith cluster; and G_i is the differential gain coefficient of the ith cluster. Auger and nonradiative recombinations are neglected because we have limited ourselves to investigations of GaAlAs–GaAs lasers in the present study. The injected current density waveform $J(t)$ is made up of a dc bias current density and an RF sinusoidal modulation signal. Its form is expressed as

$$J(t) = J_{dc} + J_m \sin(2\pi f t) \tag{2}$$

where J_{dc} and J_m are the dc bias and modulation current densities, respectively; f is the RF modulation frequency. For the generation of the shortest mode-locked laser pulses, the modulation frequency should be detuned slightly lower than the frequency matched to the external-cavity round-trip time [20].

The rate of change of forward and backward traveling photon fluxes of the ith cluster, S_i^+ and S_i^-, are

$$\frac{\partial S_i}{\partial t} \pm v_g\frac{\partial S_i}{\partial x} = \Gamma G_i[N(x,t)-N_0]S_i^{\pm}(x,t) - v_g\alpha_{\text{tot}}S_i^{\pm}(x,t) + \Gamma K_i BN^2(x,t) \tag{3}$$

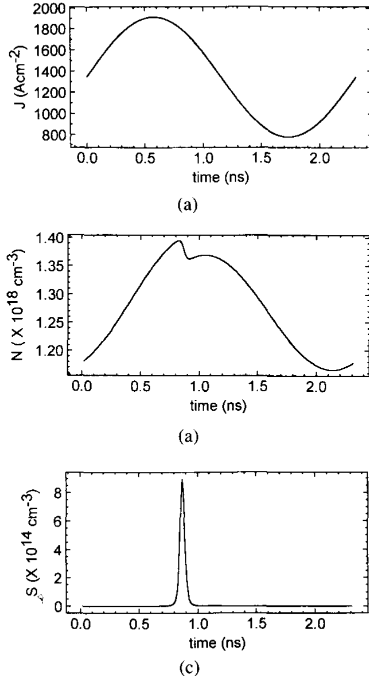

Fig. 2. Calculated waveforms over one period of (a) current density, (b) the carrier density at the AR-coated facet, and (c) photon density emitting from the AR-coated facet.

where Γ is the optical confinement factor; $v_g = c/n, n$ is the group refractive index of the laser medium; c is the velocity of light in air; and K_i is the fraction of spontaneous emission that is coupled into the two counter propagating photon fluxes of the ith cluster. The total internal loss of the active region, α_{tot}, is

$$\alpha_{\text{tot}} = \alpha_{fa}\Gamma N + \alpha_{\text{scat}} + (1 - \Gamma)\alpha_{ca} \tag{4}$$

where α_{fa} is the free-carrier absorption coefficient within the active region; α_{scat} is the coefficient of scattering loss at the interfaces of the heterostructure; and α_{ca} is the absorption coefficient of the cladding-layer.

As a first approximation and following previous workers [21], we assume the line shape factors for gain and spontaneous emission are Lorentzian with the same half width. The individual longitudinal modes within the ith cluster of the spectral distribution are assumed to possess identical gain and spontaneous emission coefficients, G_i and K_i respectively:

$$G_i = G_0 \frac{1}{1 + \left(\frac{\lambda_i - \lambda_0}{\Delta\lambda_g}\right)^2} \tag{5}$$

and

$$K_i = K_0 \frac{1}{1 + \left(\frac{\lambda_i - \lambda_0}{\Delta\lambda_g}\right)^2} \tag{6}$$

where λ_0 is the central wavelength at which the gain and spontaneous-emission coefficients exhibit their maximum values of G_0 and K_0, respectively; λ_i is the central wavelength of the ith cluster; and $\Delta\lambda_g$ is the half width of the gain lineshape.

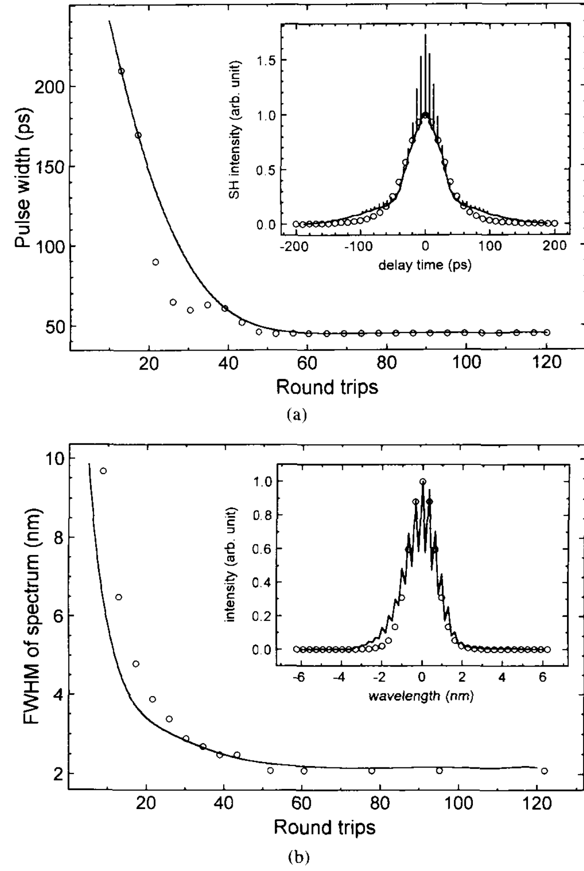

Fig. 3. (a) Pulse width as a function of delay time. Open circles are experimental data. The inset shows an autocorrelation trace of the steady state pulse (solid line) and calculated result (open circles). (b) Spectral bandwidth as a function of delay line. Open circles are experimental data. The inset shows experimentally observed steady-state spectrum (solid curve) and calculated result.

To solve the coupled rate equations, we specify the following boundary conditions:

$$S_i^+(0, t) = S_i^-(0, t). \tag{7}$$

$$S_i^-(l_d, t) = S_i^+(l_d, t)R_a + S_i^+(l_d, t - \tau_{\text{ext}})RC_c(1 - R_a) \tag{8}$$

and

$$S_i^-(L, t) = S_i^+(L, t)R \tag{9}$$

where l_d is the length of laser diode; L is the length of the external resonator; R_a is the power reflectivity of the AR-coated chip-facet; R is the power reflectivity of the output mirror; C_c is the coupling efficiency of laser light from the external cavity back into the laser diode; and τ_{ext} is the external-cavity round-trip time.

To investigate the pulse buildup dynamics of the actively mode-locked laser diode array, we solved equations (1)–(9) numerically by using the Runge–Kutta fourth-order procedure. Actual experimental parameters [16] wherever applicable were adopted. To summarize briefly, the laser diode chip was

TABLE I

variable	symbol	value	unit
Lasing wavelength	λ_0	0.8	μm
Active region thickness	d	0.1	μm
Radiative recombination coefficient	B	$5x10^{-10}$	cm^3s^{-1}
Transparency carrier coefficient	N_0	$1.2x10^{18}$	cm^{-3}
Optical confinement factor	Γ	0.5	
Group refractive index	n	4.3	
Free-carrier absorption coefficient	α_{fa}	$5x10^{-18}$	cm^2
Scattering loss coefficient	α_{scat}	5	cm^{-1}
Cladding-layer absorption coefficient	α_{ca}	10	cm^{-1}
Laser diode chip length	l_d	250	μm
External cavity length	L	34.6	cm
rf modulation frequency	f	432.1	MHz
Maximum gain coefficient	G_0	$5x10^{-6}$	cm^3s^{-1}
Maximum spontaneous emission factor	K_0	$1x10^{-6}$	
Power reflectivity of the output mirror	R	0.4	
Power reflectivity of the AR-coated facet	R_a	$1x10^{-4}$	
Half width of the gain lineshape	$\Delta\lambda_g$	50	nm
dc bias current	I_{dc}	$0.9I_{th}$	
rf modulation current	I_m	$0.38I_{th}$	
# of clusters of longitudinal modes	M	20	

a commercial 10-stripe device (Spectra Diode Labs, model SDL$-2419C, \lambda = 0.81\mu m$). It had a HR coating of $\approx$ 95% on the back facet and an AR coating of $\approx$ 0.1% on the front facet, which is imaged by a $20\times$, 0.5-N.A. objective lens and a cylindrical lens (f = 150 mm) onto the output mirror (R = 40%). The optimum dc bias current for generating the shortest *single pulses* was 250 mA or $0.9I_{\rm th}(I_{\rm th} = 260$ mA). The laser was simultaneously injected with an rf modulation current, $I_m \approx 0.38I_{\rm th}$, generating $\approx$1 W of peak power at 433 MHz. The external cavity length , L $\approx$34.6 cm. Reasonable values for other variables (see Table I) used in the equations are taken from the literature [11], [22], as experimental values are not available. In the numerical calculation, the laser diode chip with l_d = 250 μm is spatially divided into a grid with a typical spacing of 83.33 μm. For each time step, new values of electron density and the two counter propagating photon fluxes are calculated for each point within the laser diode.

III. Results And Discussions

Calculated time dependence of the steady-state photon and carrier densities over one period of the modulation signal are shown in Fig. 2. The dc and RF current densities (J_{dc} = 0.9 $J_{\rm th}$ and J_m = 0.38 $J_{\rm th}$) are experimental parameters required for the generation of the shortest *single* pulses. We find that the carrier density lags the sinusoidal current density by a phase delay of 0.55 rad. It can also be seen that the carrier density is abruptly saturated to a value below threshold right after the peak of the optical pulse. The steady-state pulse width (FWHM) is $\approx$45 ps, assuming a Gaussian pulse shape. The corresponding autocorrelation trace is in good agreement with the experimental data which are both shown in the inset of Fig. 3(a).

A. Evolution of Pulse Width and Spectrum

In Fig. 3(a), we present numerical results for the transient pulse widths of the actively mode-locked external-cavity laser diode array as a function of delay time. Zero delay time corresponds to the onset of diode laser action. The results are in good agreement with our experimental observations [16]. Qualitatively, the buildup can be described as follows: The primary pulse-shortening force for this laser is gain saturation. Since the dc bias was below the threshold, initially there was only spontaneous emission inside the cavity. After the modulation signal was turned on, a train of weakly modulated optical pulses would appear. As these weak pulses circulated inside the cavity, the central regions of the pulses would experience more gain than their wings. As a result, the pulse shape sharpened as the pulse train evolved to the steady state. During the first 15 to 20 round-trips, the pulse width shortened quickly due to rapid gain saturation and approached the steady state in approximately 45 round-trips.

Experimental data and calculated results of the bandwidth, $\Delta\lambda$, of the pulse spectrum as a function of the delay time is shown in Fig. 3(b). It can be seen that $\Delta\lambda$ narrowed quickly during the initial stage of the buildup ($\approx$40 ns or 15 to 20 round-trips) and reached the steady state also in approximately 100 ns or 45 round-trips. The steady-state spectrum is shown in the inset. The spacing of the clusters of longitudinal modes is $\approx$0.3 nm, corresponding to a chip length of 250 μm with a group velocity, $v_g \approx c/4.3$. This can be explained by the following: During the initial stage of the pulse formation, several diode chip modes would lase. These unlocked modes translated into random and fast fluctuations in time and longer pulse durations. After a few round-trips, the pulses shapes monotonously shortened and cleaned up. At the same time, the number of clusters in the spectrum would also decrease owing to the effect of competition among the clusters in a primarily homogeneously broadened medium. Finally, the pulses approached the steady state with the energy of the entire pulse distributed among a few clusters of the longitudinal modes of the chip cavity near the line center. As the pulses shorten, we also expect the bandwidth of each of the clusters to broaden. These could not be confirmed at this time, however, due to the resolution limit of the experiment.

B. Parametric Study of the Buildup

The transient pulse width characteristics of the mode-locked laser are found to vary with the laser parameters, e.g., the dc bias current (I_{dc}), rf modulation current (I_m), spontaneous emission factor (K), gain coefficient (G), radiative recombination coefficient (B), output-mirror power reflectivity (R), and the power reflectivity of the AR-coated front facet of the laser diode chip (R_a). The effects of these parameters on pulse buildup dynamics are investigated theoretically by changing one of the laser parameters while keeping the others constant to find out the effect of each of the parameters on the pulse

buildup time and the normalized pulse- shortening speed. The latter is defined as, $v_{ps} \equiv |(\tau_n - \tau_{n-1})/\tau_n|$, where $\tau_n$and τ_{n-1} are the transient pulse width at the end of the nth and $(n-1)$th round-trip, For the results presented below, we show data for the pulse-shortening speed at a delay for which $\tau_n \approx 200$ ps, i.e., $\hat{v}_{ps} \equiv (v_{ps})_{\tau_n \approx 200ps}$. This delay corresponds, for our laser, to an early stage in the pulse evolution process at which the pulse width shortens rapidly (see Fig. 3(a)).

1) DC biased Current: The effect of changing the dc bias current on the steady-state pulse width, τ_{ss}, and the buildup time, $\Delta T_{\text{buildup}}$, are illustrated in Fig. 4(a). It can be seen that the steady-state pulse width shortens abruptly from ≈340 ps to ≈100 ps while the buildup time increases from ≈15 to 60 round-trips as I_{dc} increases slightly from 0.85 I_{th} to 0.87 I_{th}. For 0.87 $I_{\text{th}} \leq I_{\text{dc}} \leq$ 0.92 I_{th}, the trend for $\tau_s s$ continues but $\Delta T_{\text{buildup}}$ reaches the maximum value for $I_{dc} \approx 0.87$ I_{th} and decreases as I_{dc} increases further. For $I_{dc} \geq 0.92$ I_{th}, the laser output consists of a train of double- or triple-pulses. In the regimes for multiple pulses (regimes (II) and (III) in Fig. 4(a) and marked with dashed vertical line in Fig. 4(a)), the durations of the first peak of the multi- pulse waveforms are shown. The steady-state pulse width varies little in these regimes while the buildup time reduces slightly. The dc bias current dependence of the pulse width can be explained as follows: As the dc bias current is increased, the carrier inversion as well as the level of gain saturation will be elevated. As a result, the laser exhibits a shorter pulse width. The strong gain saturation of the leading edge of the pulse also moves the pulse to the earlier part of the modulation period. For a current waveform with relatively long duration, such as the case for our laser, the active medium therefore will still have enough gain for generating the second and third pulse.

The buildup behavior can be understood by analyzing the normalized pulse shortening speed, $\hat{v}_{ps}$, as a function of the dc bias current. This is shown in Fig. 4(b). We find that $\hat{v}_{ps}$ monotonously increases as the dc bias current increases. This trend can also be attributed to the effect of gain saturation. For $I_{\text{dc}} \geq 0.88$ I_{th}, since the steady-state pulse width of the laser only changes slightly as I_{dc} varies, faster $\hat{v}_{ps}$ means that the initial rapidly varying portion of the buildup (see Fig. 3(a)) is shorter at higher I_{dc}. As a result, evolution from noise burst to essentially the same steady state pulse width takes less time. For $I_{\text{dc}} < 0.88$ I_{th}, however, gain is saturated to a lesser degree. The pulse shortening speeds are relatively small and not significantly different as I_{dc} varies. It simply takes less time for the mode-locked laser to evolve, if the steady-state pulse pulse width is broader.

2) RF Modulation Current: Both the steady-state pulse width and the buildup time as a function of the RF modulation current are shown in Fig. 5(a). The steady-state pulse width monotonously decreases as the RF modulation current is increased from 0.31 to 0.5 I_{th}. The buildup time to the steady state is also shortened from 67 to 42 round-trips. The general trend is similar to that predicted for the dependence of the pulse width on I_{dc}. The effect of increasing the RF modulation current on shortening of the pulse width and the buildup time can also be attributed to higher level of gain saturation.

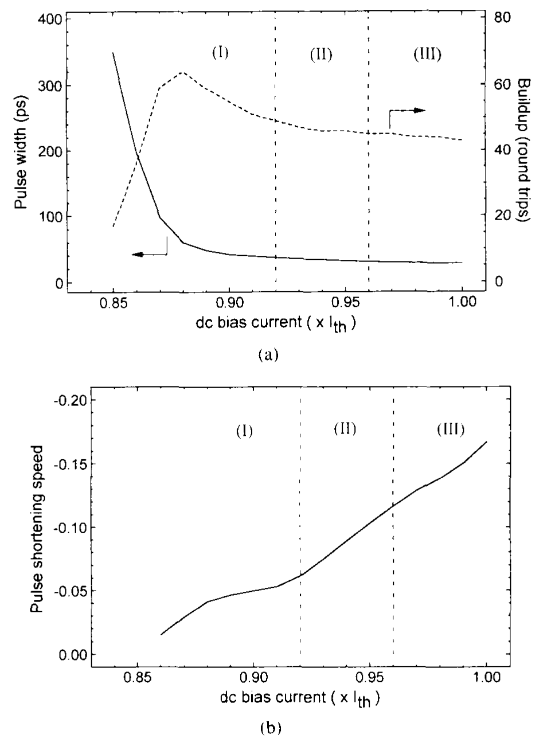

Fig. 4. Calculated dependence of (a) the steady-state pulse width and buildup time and (b) normalized pulse shortening speed on dc bias current of the laser.

Our results are consistent with calculated dependence of the steady-state pulse width dependence on I_m by Bowers *et al.* [13].

In Fig. 5(b), we show that for ≈50% change in the RF modulation current, the pulse shortening speed, $\hat{v}_{ps}$, increases less than three times. In comparison, for less than 20% change in I_{dc}, the corresponding change in $\hat{v}_{ps}$ is 17 fold (see Fig. 4(b)). Thus the RF modulation current has a smaller effect on the buildup time and the steady-state pulse width than the dc bias current. Therefore, to ensure that an actively mode-locked semiconductor laser generates the shortest possible optical pulse width or fastest buildup, one must adjust the dc bias current more carefully than the RF modulation current.

3) Radiative Recombination Coefficient: In Fig. 6(a), we display both the steady-state pulse width and the buildup time as a function of the radiative recombination coefficient, B, or the inverse of the carrier (upper state) life time, $\tau = 1/BN$. It is apparent from this figure that the steady-state pulse width rapidly shortens from ≈320 ps to ≈80 ps as B increases from 3.4 $\times 10^{-10}$ to 4 $\times 10^{-10}$ cm^3 s^{-1} and then decreases more slowly to ≈25 ps as the B coefficient increases from 4 $\times 10^{-10}$ up to 7 $\times 10^{-10}$ cm^3 s^{-1}. The buildup time versus B curve exhibits a broad peak at 4 $\times 10^{-10}$ cm^3 s^{-1}. The normalized pulse shortening speed, $\hat{v}_{ps}$, however, monotonously increases with the radiative recombination coefficient, as shown in Fig. 6(b). These trends can be qualitatively described as follows: For an actively mode-locked semiconductor laser in an external cavity, the repetition rate of the laser pulse train is fixed by keeping the external cavity length a constant.

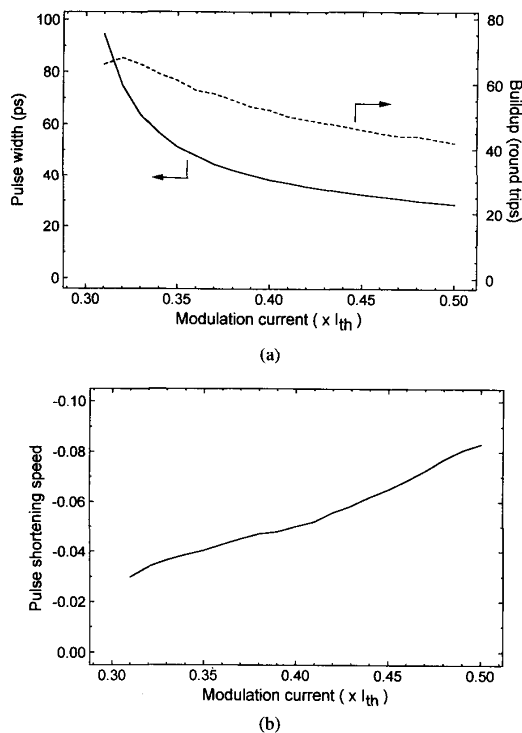

Fig. 5. Calculated dependence of (a) the steady-state pulse width and buildup time and (b) normalized pulse shortening speed on RF modulation current of the laser.

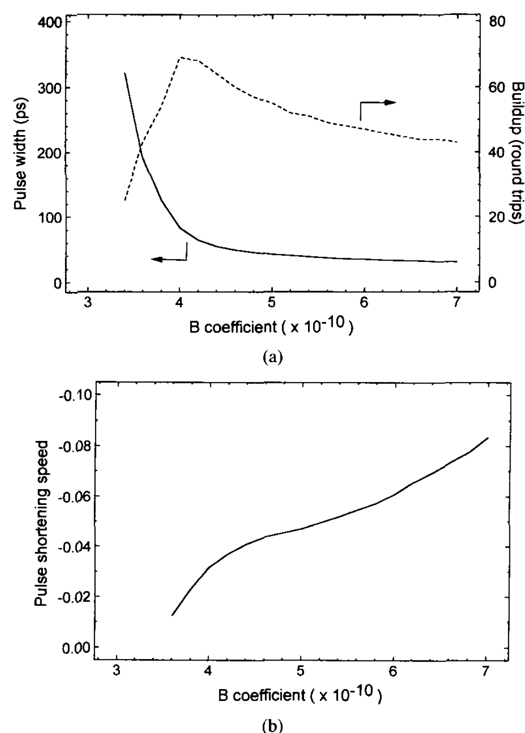

Fig. 6. Calculated dependence of (a) the steady-state pulse width and buildup time and (b) normalized pulse shortening speed on the radiative recombination coefficient.

Because of the high level of gain saturation, the carrier density of the diode laser will be periodically burnt up and depleted down to the threshold in each round-trip of the optical pulse (as shown in Fig. 2). In order to sustain the mode locked pulse train, the inversion of carriers should be sufficiently recovered for the next round-trip for pulse amplification. If the laser diode exhibits a shorter carrier lifetime, corresponding to a larger B coefficient, the higher degree of recovery of the inversion will allow the next pulse to sufficiently saturate the gain. As a result, the higher the B coefficient, the shorter we expect the steady-state pulse width to be. The buildup time, on the other hand, depends both on the pulse shortening speed and the steady-state pulse width. The latter is determined by the balance of pulse shortening and broadening forces in the steady state. This picture is consistent with previous experiments [1]–[8] in which the laser medium with the shorter excited-state lifetime are found to exhibit a shorter buildup time. Although the laser systems investigated in these studies employed different types of mode locking schemes, the order of magnitudes of the reported buildup times follows the trend predicted above.

While we predict that higher radiative recombination coefficient or shorter carrier lifetime corresponds to faster evolution, this is valid only if the repetition period of the pulse train is larger than or comparable to the carrier lifetime. If the pulses get much shorter than the recombination time, chirping and dispersion effects are significant. The dependence of buildup dynamics on B coefficient might not be straightforward as predicted here. For a threshold carrier density of 1.36 $\times 10^{18}$ cm^3, the range of B coefficients from 4 $\times 10^{-10}$ to 7 $\times 10^{-10}$ cm^3 s^{-1} corresponds to carrier lifetimes between 1.84 and 1.05 ns. These carrier lifetimes are slightly shorter than the repetition period of the pulse train used in this study (2.309 ns). This explains why the pulse width varies little with the B coefficient over this range (as shown in Fig. 6(a)). For $B \leq 4 \times 10^{-10}$, the buildup time is dominated by the effect of evolution of a broader steady-state pulse. For $B > 4 \times 10^{-10}$, on the inverse-slope of the curve, the buildup time is dominated by the initial rapidly shortening of the pulses. This is analogous to the behavior predicted for the dc bias current dependence.

4) Gain Coefficient: Because gain saturation is the primary pulse shortening force in an actively mode-locked laser diode array, we expect laser structure with higher gain coefficients will generate shorter optical pulses. This effect is illustrated in Fig. 7(a). The calculated pulse width gradually shortens from 58 to 35 ps as the gain coefficient is increased from 3 $\times 10^{-6}$ to 7 $\times 10^{-6}$ cm^3 s^{-1}. In practice, there are several methods one can use to realize variation of the gain coefficient in this range, e.g., operating the laser diode at low temperature [23], GaInAsP lasers with p-type doped active region [24], or by using lower dimensional quantum structures [25]. The essentially linear gain coefficient dependence of the normalized pulse shortening speed is shown in Fig. 7(b). In this range, since the variation of the steady-state pulse widths is quite small, the pulse buildup time is dominated by the pulse shortening

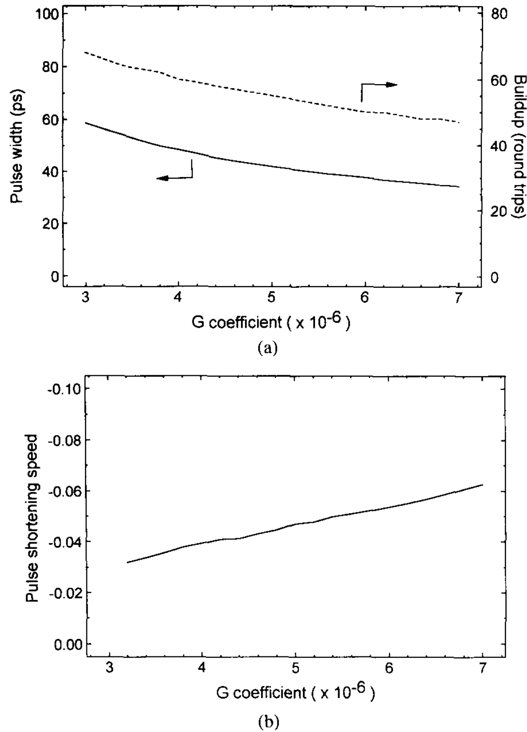

Fig. 7. Calculated dependence of (a) the steady-state pulse width and buildup time and (b) normalized pulse shortening speed on the gain coefficient of the laser.

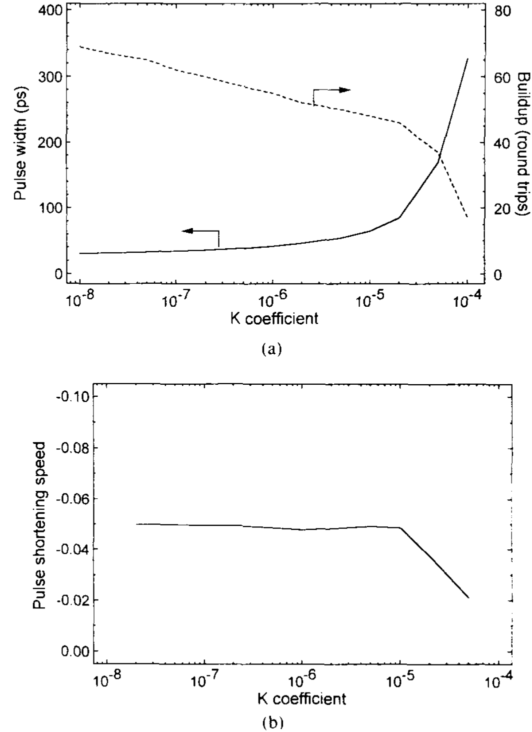

Fig. 8. Calculated dependence of (a) the steady-state pulse width and buildup time and (b) normalized pulse shortening speed on the spontaneous emission factor of the laser.

speed. As a result, the buildup time is also expected to decrease linearly with increasing gain coefficients.

5) Spontaneous Emission Factor: The spontaneous emission factor can have a large range of possible values depending on the size and structure of the semiconductor laser. The curves in Fig. 8(a) shows how the steady-state pulse width and buildup time are expected to vary with the spontaneous emission factor. It is found that the change of the pulse width is small if the spontaneous emission factor is in the range from 10^{-8} to 10^{-5}. As the spontaneous emission factor is increased beyond 10^{-5}, a dramatically larger steady- state pulse width is observed. This is due to the fact that increasing amount of spontaneous emission entering the lasing longitudinal modes will prevent the formation of a shorter optical pulse. The magnitude of spontaneous emission factor has little effect on the pulse shortening speed over a wide range of K from 10^{-8} to 10^{-5}. For $K \geq 10^{-5}, \hat{v}_{ps}$ monotonously decreases. This is shown in Fig. 8(b). As a result, for lasers with larger K coefficients, we predict broader steady-state pulse widths and correspondingly shorter buildup time.

6) Power Reflectivities of the Output Mirror and the AR-Coated Facet: We have also studied the steady-state pulse width, temporal buildup time, and pulse shortening speed as a function of the power reflectivity of the output mirror, R, respectively. It is found that both τ_{ss} and $\Delta T_{\text{buildup}}$ versus R curves (not shown) are nearly independent of the changes in R. This implies that the buildup dynamics of an actively mode-locked laser diode array in an external cavity is not significantly affected by the magnitude of the intra cavity energy. By increasing the magnitudes of the power reflectivity of the AR-coated facet, R_a, from 10^{-4} to 10^{-2}, we also find that the temporal evolution characteristics of the laser is nearly invariant for R_a in this range.

IV. SUMMARY

An approximate theoretical analysis, based on modified traveling-wave rate equations for a single-stripe laser diode, has been developed to analyze the pulse buildup dynamics of an actively mode-locked semiconductor laser diode array in an external cavity. Good agreements with experimental observations are found for both transient and steady-state pulse width and spectral characteristics. We have also performed numerical simulation of the effects of various laser operating parameters on the pulse buildup. The parameters studied include the dc bias current, RF modulation current, radiative recombination coefficient, gain coefficient, spontaneous emission factor, output-mirror power reflectivity, and the antireflection-coated power reflectivity. We conclude that the dc bias current (or the pumping power) and the radiative recombination coefficient (or the upper state lifetime) are the dominant parameters affecting the buildup dynamics. The dependence are nonlinear, because of the saturation characteristics of the laser. The changes in the power reflectivities of the output mirror and the AR-coated facet of the diode chip have little effect on the temporal evolution characteristics, however. We expect

the predicted trend to be valid if the active medium is a single-stripe diode chip.

REFERENCES

[1] J. A. R. Williams, P. M. W. French, and J. R. Taylor, "An investigation into femtosecond pulse formation in a continuously-pumped passively mode-locked CPM ring dye laser," *IEEE J. Quantum Electron.*, vol. 26, pp. 1434–1439.

[2] J.-C. Kuo and C.-L. Pan, "Buildup of steady-state subpicosecond and femtosecond pulses in a colliding-pulse mode-locked ring dye laser," *Opt. Lett.*, vol. 15, pp. 1297–1299, 1990.

[3] J. J. Kasinski, L. A. Gomez-Jahn, R. J. Dwayne Miller, P. Geist, B. Geoffroy, F. Heisel, A. Martz, and J. A. Miehe, "Picosecond pulse formation in synchronously pumped dye lasers," *J. Opt. Soc. Am. B*, vol. 3, pp. 1566–1572, 1986.

[4] J. Goodberlet, J. Wang, and J. G. Fugimoto, "Starting dynamics of additive-pulse mode locking in the $Ti:Al_2O_3$ laser," *Opt. Lett.*, vol. 16, pp. 1180–1182, 1990.

[5] N. Sarukura and Y. Ishida, "Pulse evolution dynamics of a femtosecond passively mode-locked Ti:sapphire laser, *Opt. Lett.*, vol. 17, pp. 61–63, 1992.

[6] J.-C. Kuo, J.-M. Shieh, C. D. Hwang, C.-S. Chang, C.-L. Pan and K.-H. Wu, "Pulse-forming dynamics of a cw passively mode-locked Ti:sapphire/DDI laser, *Opt. Lett.*, vol. 17, pp. 334–336, 1992.

[7] K. P. J. Reddy and J. A. Tatum, "Dynamics of active mode locking in broad-band continuous wave lasers," *IEEE J. Quantum Electron.*, vol. 29, pp. 1407–1411, 1993.

[8] S. Ruan, J. M. Sutherland, P. M. W. French, J. R. Taylor, P. J. Delfyett, and L.T. Florez, "Pulse evolution in cw femtosecond $Cr^3+: LiSrAlF_6$ lasers mode-locked with MQW saturable absorbers," *Opt. Commun.*, vol. 110, pp. 340–344, 1994.

[9] O. Solgaard, M.-H. Kiang, and K. Y. Lau, "Pulse buildup in passively mode-locked monolithic quantum-well semiconductor lasers," *Appl. Phys. Lett.*, vol. 63, pp. 2021–2023, 1993.

[10] J. C. AuYeung, L. A. Bergman, and A. R. Johnson, "Transient-behavior of an actively mode-locked semiconductor-laser Diode," *Appl. Phys. Lett.* vol. 41, no. 2, pp. 124–126, 1982.

[11] M. S. Demokan, "A model of a diode laser actively mode-locked by gain modulation," *Int. J. Electron.*, vol. 60, pp. 67–85, 1986.

[12] P. Blixt and A. Krotkus, "Simulations and experiments of mode-locking of semiconductor lasers: pulse evolution, frequency detuning and bias dependence," *Opt. and Quantum Electron.*, vol. 22, pp. 561–570, 1990.

[13] J. E. Bowers, P. A. Morton, A. Mar, and S. W. Corzine, "Actively mode-locked semiconductor lasers," *IEEE J. Quantum Electron.*, vol. 25, pp. 1426–1439, 1989.

[14] J. P. van der Ziel, H. Temkin, R. D. Dupuis, and R. M. Mikulyak, "Mode-locked picosecond pulse generation from high power phase-locked GaAs laser arrays," *Appl. Phys. Lett.*, vol. 44, pp. 357–359, 1984.

[15] H. Masuda and A. Takada, "Picosecond optical pulse generation from mode-locked phased laser diode array," *Electron. Lett.*, vol. 25, pp. 1418–1419, 1989.

[16] J.-C. Kuo, C.-S. Chang, and C.-L. Pan, "Buildup of steady-state picosecond pulses in an actively mode-locked laser-diode array," *Opt. Lett.*, vol. 16, pp. 1328–1330, 1991.

[17] S. S. Wang and H. G. Winful, "Dynamics of phase-locked semiconductor laser arrays," *Appl. Phys. Lett.*, vol. 52, pp. 1774–1776, 1988.

[18] A. J. Lowery, "Modeling spectral effects of dynamic saturation in semiconductor laser amplifiers using the transmission-line laser model," *Inst. Elect. Eng. Proc.*, vol. 136, pt. J, pp. 320–324, 1989.

[19] G. P. Agrawal and N. A. Olsson, "Self-phase modulation and spectral broadening of optical pulses in semiconductor laser amplifiers," *IEEE J. Quantum Electron.*, vol. 25, pp. 2297–2306, 1989.

[20] J. C. Goodwin and B. K. Garside, "Modulation detuning characteristics of actively mode-locked diode lasers, *IEEE J. Quantum Electron.*, vol. QE-19, pp. 1068–1073, 1983.

[21] D. Marcuse and T.-P. Lee, "On approximate analytical solutions of rate equations for studying transient spectra of injection lasers, *IEEE J. Quantum Electron.*, vol. QE-19, pp. 1397–1406, Sept. 1983.

[22] N. Yu, R. K. DeFreez, D. J. Bossert, G. A. Wilson, R. A. Elliott, S.-S. Wang, and H. G. Winful, "Spatialspectral and picosecond spatiotemporal properties of a broad area operating channeled-substrate-planar laser array," *Appl. Opt.*, vol. 30, no. 18, pp. 2503–2513, 1991.

[23] K. Y. Lau, C. Harder, and A. Yariv, "Direct modulation of semiconductor lasers at $f > 10$ GHz by low temperature operation," *Appl. Phys. Lett.* vol. 44, pp. 273–275, 1984.

[24] C. B. Su and v. Lanzisera, "Effect of doping level on the gain constant and modulation bandwidth of semiconductor lasers, *Appl. Phys. Lett.*, vol. 45, pp. 1302–1304, 1984.

[25] K. Uomi, N. Chinone, T. Ohtoshi, and T. Kajimura, "High relaxation oscillation frequency (beyond 10 GHz) of GaAlAs multi-quantum well lasers," *Jpn. J. Appl. Phys.*, vol. 24, pp. 539–541, 1985.

Chi-Luen Wang, biography and photograph not available at time of publication.

Jahn-Chung Kuo, biography and photograph not available at time of publication.

C.-S. Chang, biography and photograph not available at time of publication.

Ci-Ling Pan, biography and photograph not available at time of publication.